Fuel 262 (2020) 116501

Contents lists available at ScienceDirect

Fuel

journal homepage: www.elsevier.com/locate/fuel

Full Length Article

The effects of Fe_2O_3 based DOC and SCR catalyst on the exhaust emissions of diesel engines

Ibrahim Aslan Resitoglu[a,*], Kemal Altinisik[b], Ali Keskin[c], Kasim Ocakoglu[d]

[a] Department of Automotive Technology, Mersin University, Technical Sciences Vocational School, TR-33343 Mersin, Turkey
[b] Department of Mechanical Engineering, Selcuk University, Engineering Faculty, TR-42030 Konya, Turkey
[c] Department of Automotive Engineering, Cukurova University, Engineering and Architecture Faculty, TR-01330 Adana, Turkey
[d] Department of Energy Systems Engineering, Faculty of Technology, Tarsus University, 33400 Tarsus, Turkey

ARTICLE INFO

Keywords:
Hematite
Diesel engine
Pollutant emissions
DOC
SCR

ABSTRACT

The effects of Fe_2O_3 based DOCs (Diesel Oxidation Catalyst) and SCR (Selective Catalytic Reduction) catalysts on the exhaust emissions of diesel engine were investigated in this experimental study. The investigated catalysts, Al_2O_3 – $TiO_2/CeO_2/Fe_2O_3$ (ATCF) and Al_2O_3 – $Nb_2O_5/CeO_2/Fe_2O_3$ (ANCF), were produced with impregnation method and aged for 6 h at 600 °C. FE-SEM (Field Emission Scanning Electron Microscopy), XRD (X-Ray Diffraction), XRF (X-Ray Fluorescence) and BET (Brunauer-Emmett-Teller) Surface Area analyzes were carried out to determine the specifications of catalysts. The catalytic performances of the DOCs were tested for the oxidation of CO, HC, PM, NO while SCR catalysts were tested for SCR of NO_x using NH_3. An individual exhaust system was built up and mounted to the engine for tests of catalysts. An electronic control system and a software were developed to control the SCR system. After the completion of experimental setup, catalysts placed inside the exhaust system were subjected to the engine tests to determine their effects on the exhaust emissions. Tests were carried out under actual working conditions with a single cylinder direct injection diesel engine. In conclusion, the catalysts made significant decrease in pollutant emissions while brake specific fuel consumption (BSFC) increased slightly. ANCF released better conversion efficiency in all pollutant emissions compared to the ATCF. Maximum decreases in CO, HC and NO_x emissions, which are resulted from ANCF catalyst, were obtained at a rate of 83.51%, 80.83% and 80.29% respectively.

1. Introduction

Serious environmental and health problems that caused by air pollution have become a common problem not only in developing countries but also around the world [1]. Pollution emissions such as CO, HC, NOx and PM in vehicles used in the transport industry have contributed significantly to the air pollution, and governments have focused on the need to reduce these pollutants [2,3]. Compression ignition (CI) engines have a greater contribution to the air pollution, especially for NO_x and PM emissions, due to their widespread use compared to spark-ignition (SI) engines. [4–6]. Pollutants from CI engines caused air pollution are carcinogenic to humans [7,8]. Many technologies (exhaust gas recirculation, electronic controlled fuel injection, crankcase ventilation, etc.) have been developed to control the pollutant emissions from CI engines. However, these technologies could not reduce the pollutant emissions to the values determined by the standards such as Euro, Tier, Japan etc. [2]. It is possible to meet the strict emission limits with the exhaust aftertreatment systems (EAS) [9]. The use of EAS in vehicles reduces pollutant emissions completely or at a high rate. The most of EAS used in diesel engines are Diesel Oxidation Catalysts (DOC), Diesel Particulate Filter (DPF) and Selective Catalytic Reduction (SCR) [3]. Each system can be used alone, or combined to increase conversion efficiency of pollutant emissions [10,11].

The DOC is used to remove CO and HC emissions at a high rate, shortly after the exhaust manifold (Eqs. (1.1) and (1.2)) [12,13]. In addition, the DOC transforms the NO in NO_2 forms to enhance the efficiency of the DPF and SCR system (Eq. (1.3)) [11].

$$CO + 1/2O_2 \rightarrow CO_2 \quad (1.1)$$

$$C_3H_6 + 9/2O_2 \rightarrow 3\,CO_2 + 3H_2O \quad (1.2)$$

$$NO + 1/2\ O_2 \rightarrow NO_2 \quad (1.3)$$

Exhaust gas temperature is very important factor in DOC conversion efficiency. The oxidations of HC and CO need a temperature called

* Corresponding author.
E-mail address: aslanresitoglu@mersin.edu.tr (I.A. Resitoglu).

https://doi.org/10.1016/j.fuel.2019.116501
Received 24 July 2019; Received in revised form 1 October 2019; Accepted 23 October 2019
Available online 06 November 2019

Nomenclature

A	Cordierite ($2Al_2O_3$-$5SiO_2$-2MgO)
Al_2O_3	Aluminum Oxide
ANCF	Al_2O_3 – $Nb_2O_5/CeO_2/Fe_2O_3$
ATCF	Al_2O_3 – $TiO_2/CeO_2/Fe_2O_3$
BET	Brunauer-Emmett-Teller
BP	Brake Power (kW)
BSFC	Brake Specific Fuel Consumption (g/kWh)
C_3H_6	Propene
CaO	Calcium Oxide
CeO_2	Cerium Dioxide
CI	Compression Ignition
CO	Carbon Monoxide
CO_2	Carbon Dioxide
DOC	Diesel Oxidation Catalyst
DPF	Diesel Particulate Filter
EAS	Exhaust Aftertreatment Systems
ER	Engine Results without Catalyst
Fe	Iron
FE-SEM	Field Emission Scanning Electron Microscopy
Fe_2O_3	Iron (III) Oxide (Hematite)
H_2O	Water
HC	Hydrocarbon
HNCO	Isocyanic Acid
K_2O	Potassium Oxide
MgO	Magnesium Oxide
NaO	Sodium Monoxide
Nb_2O_5	Niobium Pentoxide
$(NH_2)_2CO$	Urea
NH_3	Ammonia
NO	Nitrogen Oxide
NO_2	Nitrogen Dioxide
NO_3	Nitrate
NO_x	Nitrogen Oxides
O_2	Oxygen
P_2O_5	Phosphorus Pentoxide
Pd	Palladium
PM	Particulate Matter
Pt	Platinum
Rh	Rhodium
SCR	Selective Catalytic Reduction
SI	Spark Ignition
SiC	Silicon Carbide
SiO_2	Silicon Dioxide
SO_3	Sulphur Trioxide
TiO_2	Titanium Dioxide
ULSD	Ultra Low Sulphur Diesel
V_2O_5	Vanadyum Pentoksit
WO_3	Tungsten Trioksit
XRD	X-Ray Diffraction
XRF	X-Ray Fluorescence
λ	Excessive Air Factor

"light off temperature". This temperature depends on the exhaust gas and catalyst type. Platinum (Pt) has conventionally been the preferred catalyst recently for DOC while Palladium (Pd) and Rhodium (Rh) have been used as alternative catalysts to Pt [3]. However, these materials are in the precious metal group and cause an increase in the cost of catalyst.

The DPF is used as a filter to eliminate PM emissions in exhaust gas. The DPF is generally made of Silicon Carbide (SiC) [12]. To ensure filtration, each cell is blocked regularly at the end. This blocked cell does not allow the exhaust flow and direct it into porous substrate wall to be gone out from DPF by filtering PM emissions. However the porous substrate wall becomes plugged in the long run. To avoid this situation, DPF must be regenerated at certain time intervals. Particles in the cell are burned at the high temperatures with active or passive regeneration [3].

The NO_x formation in the exhaust gas can be removed by a reductant in the SCR system [6]. While, different reductants have been reported such as alcohol, hydrocarbons, hydrogen, etc.; Ammonia (NH_3) showed better performance as a reductant in SCR [14,15]. To prevent NH_3 from burning at the high exhaust temperatures, ammonia is obtained from urea solution in vehicular applications [16]. The reactions occurred in the SCR systems are given in Eqs. (1.4)–(1.8) [17].

$$(NH_2)_2CO \rightarrow NH_3 + HNCO \,(\text{thermolysis}) \quad (1.4)$$

$$HNCO + H_2O \rightarrow NH_3 + CO_2 \,(\text{hydrolysis}) \quad (1.5)$$

$$4NO + 4NH_3 + O_2 \rightarrow 4N_2 + 6H_2O \quad (1.6)$$

$$2NO + 2NO_2 + 4NH_3 \rightarrow 4N_2 + 6H_2O \quad (1.7)$$

$$6NO_2 + 8NH_3 \rightarrow 7N_2 + 12H_2O \quad (1.8)$$

As soon as the urea solution is sprayed over the exhaust gas, thermolysis and hydrolysis reaction occur to release NH_3. [15,18]. After thermolysis and hydrolysis, the reactions of NO_x with urea can occurs in three different ways (Eqs. (1.6)–(1.8)) according the state of NO:NO_2 rate. The reaction at the Eq. (1.7), between the reactions, has the most conversion efficiency due to high conversion rate [18]. The most common type of SCR catalyst used in mobile applications is V_2O_5-WO_3/TiO_2 structures because of its high thermal stability and conversion efficiency [6,18,19]. However, the toxicity of vanadium-based catalyst may be detrimental for environment and human health [19].

In this experimental study, hematite, found as widely in nature and had a high catalyst effect in addition of its low cost was investigated as an alternative base material in DOC and SCR catalyst. Titanium, cerium, and niobium complex were added in the catalyst solution to increase the activation. Catalysts were tested under actual working conditions with a single cylinder direct injection diesel engine. The effect of Hematite-based catalysts on not only pollution emissions but also on BSFC, excessive air factor (λ), O_2, CO_2 and exhaust gas temperature was investigated experimentally.

2. Material and methods

2.1. Preparation of the catalysts

The flow diagram of catalyst production is illustrated in Fig. 1. Two different catalysts as Al_2O_3 – $TiO_2/CeO_2/Fe_2O_3$ (ATCF) and Al_2O_3 – $Nb_2O_5/CeO_2/Fe_2O_3$ (ANCF) were produced by impregnation method. The cordierite ($2Al_2O_3$-$5SiO_2$-2MgO) monolith, which constitutes the main structure, was obtained commercially as Ø103x55 mm and 400 cpsi with square mesh. The hematite (Fe_2O_3) sol-gel was prepared according to the previously published method [20]. To achieve two different coating solutions of catalysts, first the hematite (Fe_2O_3) solution was prepared and the additive catalyst was doped in hematite solution. $Fe(NO_3)_3x9H_2O$ (Merck) and $CH_3(CH_2)_7CH = CH(CH_2)_7COOH$ (oleic acid) were used to obtain hematite structure. Cerium (III) acetate hydrate and Titanium (IV) oxide (Alfa Aesar) were separately diffused at a rate of 3% in hematite solution to create the first (ATCF) solution. Niobium (V) chloride (Aldrich) as a rate of 3% of hematite solution and Cerium (III) acetate hydrate as twice as Niobium (V) chloride were mixed and doped in the hematite solution to form second (ANCF) solution. The main cordierite structures were doped into the solutions. After impregnation, each sample was dried in the drying furnace at

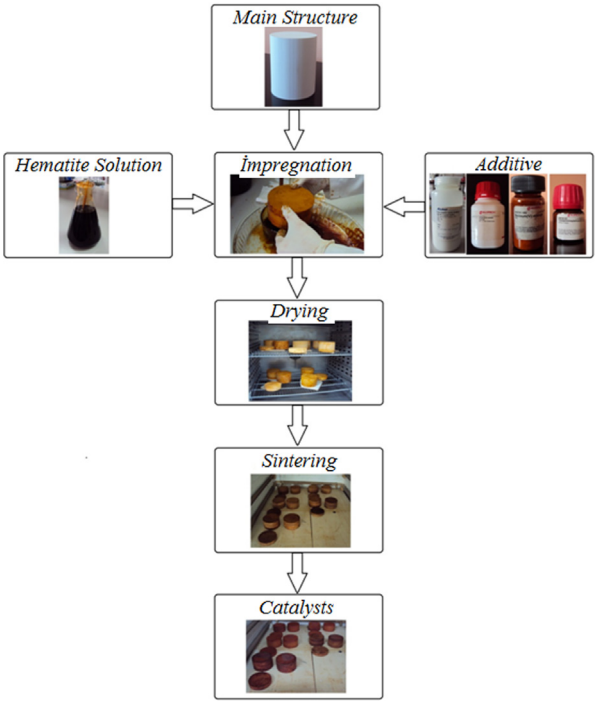

Fig. 1. Flow diagram of catalysts production.

120 °C for 12 h and sintered at 600 °C for 6 h. Finally, two pieces of ATCF and ANCF were produced and tested as DOC and SCR catalyst. Catalysts in smaller thickness were also produced to determine catalyst specifications.

2.2. Analysis of the catalysts

FE-SEM (Field Emission-Scanning Electron Microscope), XRD (X-ray diffraction), XRF (X-ray fluorescence) and BET (Brauner – Emmett – Teller) analyzes were carried out to determine the pore structure, microanalysis and crystal structure, chemical structure and the surface area of catalysts, respectively. The model of FE-SEM, BET, XRD and XRF devices were Zeiss/Supra 55, Quantachrome Nova-e, LECO/CHNS – 932, Rigaku-Smartlab, X-ray powder diffractometer and Rigaku- ZSX Primus II WD-XRF, respectively. Catalysts were pulverized by milling for BET, XRD and XRF analyzes. In addition, pellet of each sample was prepared for XRF analyzes. 10 g of powder samples and 4 g of cellulose were mixed in a pot. The prepared mixtures were pressed at 36 MPa to form pellets. The resulting pellets were analyzed after standing at 100 °C for 12 h in the oven.

2.3. Control of the SCR systems

The amount of NOx in exhaust gas and the exhaust gas velocity are two major factors to determine the urea solution sprayed on exhaust gas. Furthermore, exhaust gas temperature is considered to prevent urea decomposition in catalyst at low exhaust temperature and the self-ignition of NH_3 at high exhaust temperature.

In experimental set-up, an electronic control system was developed to control the spraying of urea solution according to the exhaust velocity and NO_x amount. The total of intake air and fuel formed the exhaust gas flow rate. Fig. 2 shows block diagram of electronic control developed for the SCR system.

Continental UniNO_x sensor, P-CAN USB, power supply, control chart, connection sockets, Pt-200 temperature sensor were used to provide electronic control of SCR. The communication between NO_x sensor, microprocessor and pump was realized with CAN J1939 protocol, while serial communication was provided with the temperature sensors. The urea solution was pumped from the urea tank to the nozzle and then injected into the gas pipe before the SCR catalyst.

2.4. Experimental setup

The drawing of experimental setup is given in Fig. 3. A single cylinder, four stroke, water cooled, direct injection Kirloskar TV1 diesel engine with a displacement of 661 cm^3, a compression ratio 18/1, 1500 rpm maximum speed and 5 kW maximum power was used in the tests. The load was established on the engine by an eddy current dynamometer. A transmitter was used before intake manifold to determine the intake airflow rate. The urea pump and injector operated as pneumatic were mounted to a compressor having 6–8 bar compressed air. A Bosch BEA-350 exhaust gas analyzer was used to measure the upstream and downstream DOC of CO, HC, PM, CO_2, O_2 and NO. Table 1 shows the specifications of the emission gas analyzer.

The tests were performed to determine the effect of DOC and SCR catalyst on the exhaust emissions. Also BSFC and λ of engine were analyzed in tests. Each of ATCF and ANCF catalyst was tested as DOC and SCR catalyst. Before the measurements, the test engine was run for 15 min to reach active temperature of both the engine and DOC. The catalysts were tested at constant engine speed (1500 d/d) with 3 Nm range between 6 and 24 Nm and 0.47 kW range between 0.94 and 3.77 kW to see the effect of catalysts on the exhaust gas. The relation between engine power output and torque is presented in Fig. 4. Ultra Low Sulphur Diesel (ULSD) was used in tests to prevent sulphur poisoning. The properties of diesel fuel used in test and EN590 standard for diesel fuel are given in Table 2. It is shown in Table that all specifications of diesel fuel are appropriate for EN590 standards.

2.5. Exhaust gas content of diesel engine with and without catalysts

This section gives the content of emissions in exhaust gas with and without catalyst. The exhaust gas content of non-catalyst engine is named as “ER”. CO, HC, CO_2, O_2, exhaust gas temperature, smoke emission, NO and NO_x values of exhaust gas with catalysts and without catalyst are presented in Fig. 5.

Compared to the ER values, the use of catalyst led to an increase in CO values at the engine output (pre-catalyst). This is because the use of catalyst increases fuel consumption and enriches the mixture. HC emissions pre-ANCF increased slightly at low torques (6–12 Nm), and decreased at high torques while HC emissions pre-ATCF showed a decrease trend in all torques compared to ER values. This situation can be explained with the low HC conversion efficiency of ANCF at low torques in the Fig. 9. CO_2 emission and O_2 content in exhaust gas showed converse effect with the use of catalyst. The CO_2 emissions increased, while O_2 content decreased compared to ER values. A significant

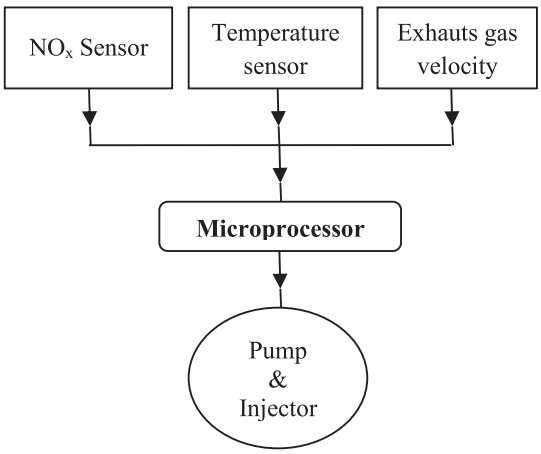

Fig. 2. Block diagram of the SCR Electronic Control System.

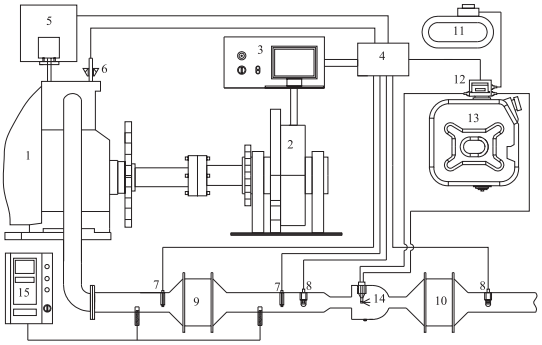

Fig. 3. A schematic representation of the experimental setup (1-Engine, 2-Dynamometer, 3-Control panel, 4-SCR control unit, 5-Fuel gauge, 6-Air flow meter, 7-Temperature sensor, 8-NO_x sensor, 9-DOC, 10-SCR catalyst, 11-Compressor, 12-Pump, 13-Urea tank, 14-Injector, 15-Emission analyzer).

Table 1
Specifications of the Bosch BEA-350 exhaust gas analyzer.

Variables	Measurement range	Resolution
CO	0–10%	0.001%
CO_2	0–18%	0.01%
HC	0–9999 ppm	1 ppm
O_2	0–22%	0.01%
λ	0.5–9.999	0.001
NO	0–5000 ppm	1 ppm
PM	0–10 m^{-1}	0.01 m^{-1}

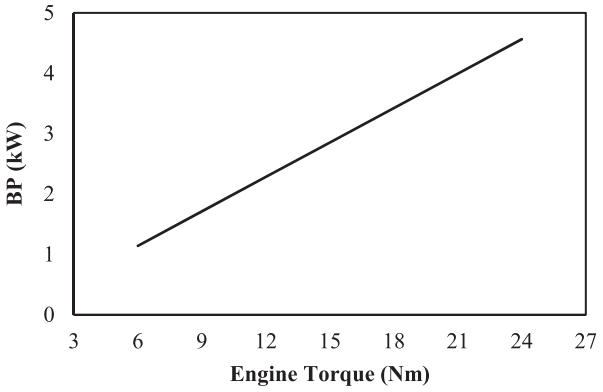

Fig. 4. The relation between engine power output and torque.

change was not obtained in exhaust temperature and Smoke emissions differed from ER values especially at high torques. NO and NO_x emissions showed an increasing trend in general compared to ER values.

3. Results and discussion

3.1. The properties of catalysts

The morphology of the prepared catalysts was determined by the Field emission-scanning electron microscopy (FE-SEM). The FE-SEM images of catalysts are given in the scale of 10 μm and 1 μm in Fig. 6.

FE-SEM images generally showed the organizations in catalysts as nano-sized. As seen in the images catalyst's surface has a porous structure on a scale of 10 μm. Homogenous coating was realized inside the pores on a scale of 1 μm. It is observed that the pores were completely covered. This showed that a good ground was prepared for the catalyst works.

The XRD graph of catalysts is given in Fig. 7. XRD results support the FE-SEM analysis results. According to the calculations, the crystallite size of the samples is around 40 nm for intensity peak (1 0 0) at $2\theta \cong 10{,}4°$. The cordierite substrate, called the graphite A, was used as template. The XRD results show that the crystallite structure of the samples is the cordierite and it has hexagonal structure with the space group of P6/mcc (1 9 2). The XRD peaks shifted to a lower angle for the ATCF and ANCF samples under the influence TiO_2, CeO_2 and Nb_2O_5 and also, the peak intensity was increased by doping of $TiO_2/CeO_2/Fe_2O_3$ and $Nb_2O_5/CeO_2/Fe_2O_3$, respectively. Thus, we can report that Nb_2O_5 is more effective than TiO_2 in increasing the crystallite structure.

The BET surface area of catalysts and the results of XRF analysis performed to determine the element ratio in the catalyst are given in Table 3. In results, Al_2O_3 and SiO_2 had biggest ratio since these structures constituted the main form of catalysts. The CeO_2 ratios in the ATCF and ANCF catalyst were measured as 0.045% and 0.174% respectively. ANCF had Nb_2O_5 complex at a rate of 0.086%. The total coating elements except for the main structural elements were 3.469% and 2.068% for ATCF and ANCF catalysts, respectively.

BET surface areas of the ATCF and ANCF catalysts were quantified as 44.649 m^2/g and 50.104 m^2/g respectively. Compared to the main structure (A), the BET surface areas of the ATCF and ANCF catalysts were considerably reduced due to penetrating of catalyst materials in pores and sintering of catalyst structures.

3.2. BSFC and λ results

Catalysts adapted to the exhaust pipe led to increase in BSFC (Fig. 8). Besides ATCF and ANCF catalyst, BSFC values of a blank cordierite monolith (A) was added in Figure. The insertion of a blank cordierite monolith raised increase of BSCF up to 15.51%. The average BSFC increase was 13.60%, 6.30% and 5.12% for A, ATCF and ANCF catalyst, respectively. The reason for the increase in the BSFC can be explained by the backpressure produced by limiting the exhaust gas passage. Compared to ATCF and ANCF, the high BSFC of A resulted from absence of catalyst and catalytic activity.

λ tended to decrease with the use of catalysts. The maximum reduction in λ was achieved as 10.81% in the ATCF catalyst at 18 Nm. While the engine λ value was 1.4 at maximum engine torque, the use of ATCF and ANCF catalyst led the λ to decrease to 1.3 and 1.38, respectively. In all tests performed, the increase in engine torque caused the decrease in λ. The increase in engine torque led to the enrichment of air/fuel mixture and the decrease of λ. Considering all engine torques, the usage of ATF and APF catalysts led to the average reduction of 5.91% and 4.77%, compared to the ER.

λ depends on air/fuel ratio taken into the cylinder. The decrease in air/fuel ratio means that the enrichment of mixture decreases the λ, otherwise the increase in air/fuel ratio leads to increase λ. Therefore, the increase of BSFC with the use of catalysts, caused to decrease in air/fuel ratio and λ.

Table 2
The properties of diesel fuel.

Fuel/Specifications	Density at 15 °C (kg/m^3)	Calorific value (MJ/kg)	Cetane number	Viscosity kinematic at 40 °C (mm^2/s)	Flash Point (°C)
Diesel	841.53	45.27	53.67	2.71	63
EN590	820–845	–	Min 51	2.0–4.5	Min 55

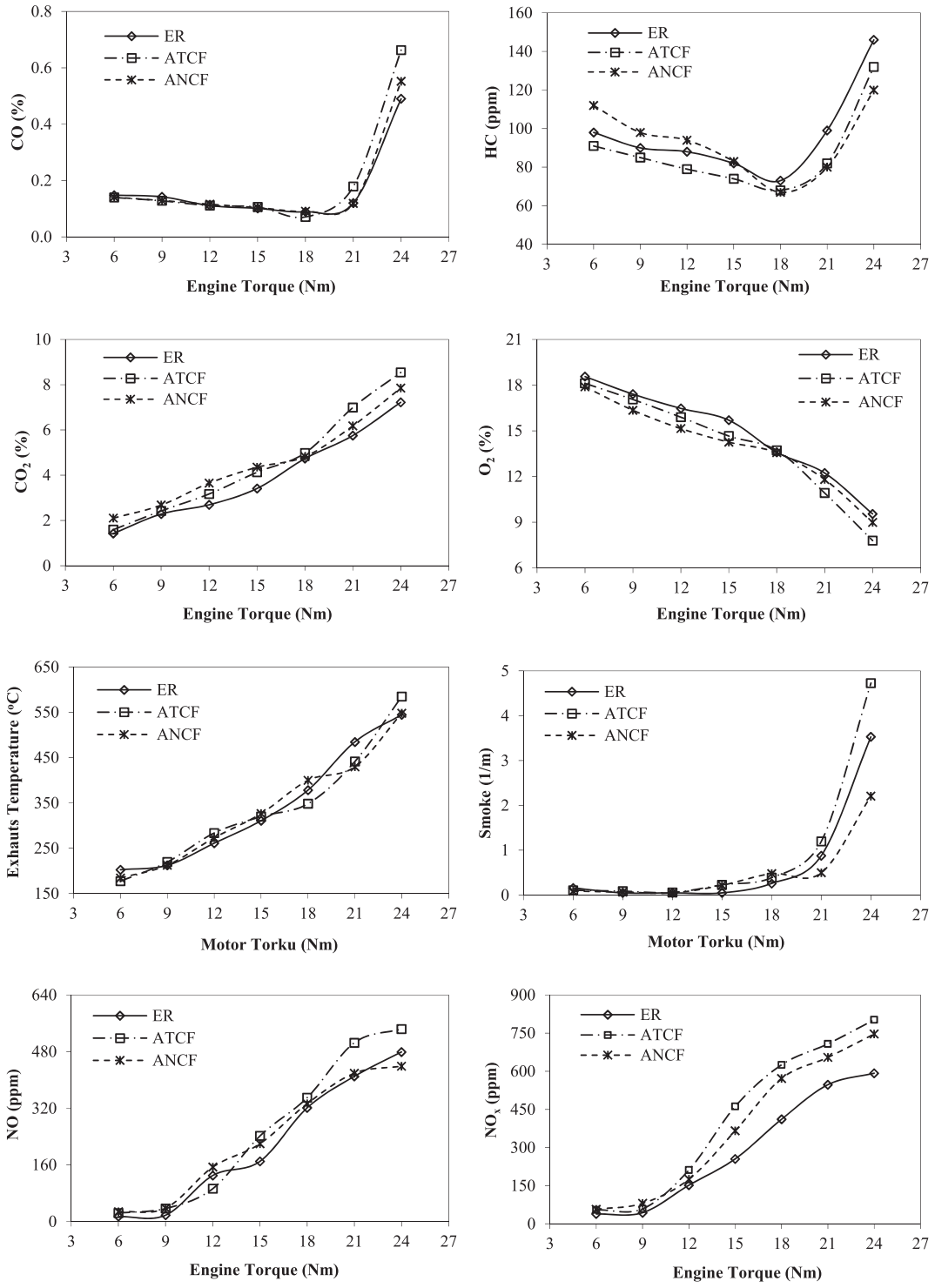

Fig. 5. Emissions of diesel engine with and without catalyst.

3.3. Engine exhaust emission results

The conversion efficiency of CO and HC emissions is given in Fig. 9. In general, ANCF showed better performance in CO and HC conversion compared to ATCF. The maximum conversion efficiency was obtained with the ANCF catalyst as 80.83% in HC conversion and 83.51% in CO conversion. ANCF catalyst led to a significant decrease in HC value with the reduction from 120 ppm to 23 ppm at 24 Nm. In low engine torque (6 and 9 Nm), the HC conversion efficiency of the ATCF was slightly higher than the ANCFs. The CO and HC conversions were averagely 46.03% and 55.92%, respectively, with the ATCF while 58.64% and 62.96% with the ANCF catalyst. The oxidation of CO and HC was increased in proportion to the increase in engine torque, which means that the exhaust temperature increases. The conversion efficiency of DOC depends largely on the temperature level of the DOC [12].

Increasing rate of CO_2 and reduction rate of O_2 are presented in Fig. 10. HC and CO molecules react with oxygen and consequently these reactions consist of CO_2 in DOC (Eqs. (1.1) and (1.2)). Hereby the O_2 content in exhaust gas decreased while CO_2 increased after the DOC. The increase rate of CO_2 and decrease rate of O_2 were changed to the

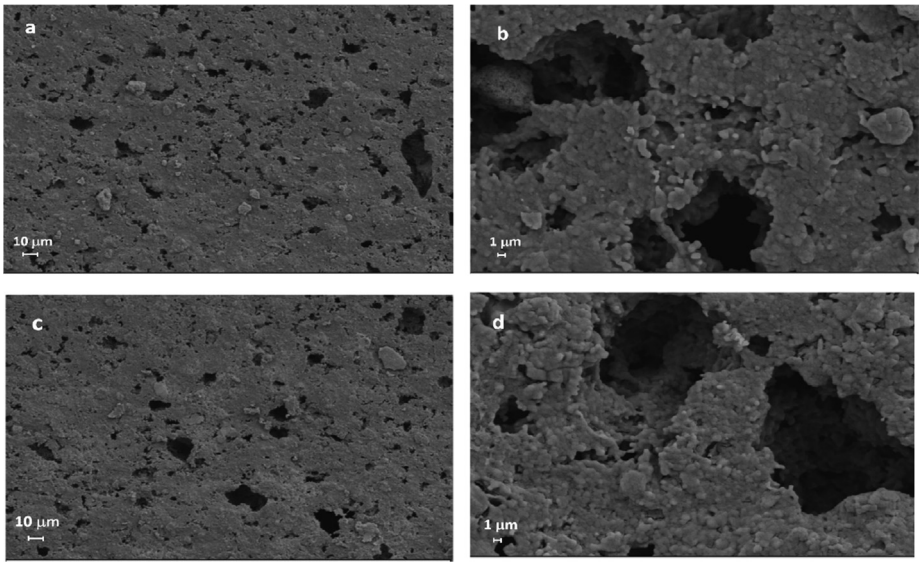

Fig. 6. FE-SEM images of the catalysts a) ATCF (10 µm), b) ATCF (1 µm) c) ANCF (10 µm) and d) ANCF (1 µm).

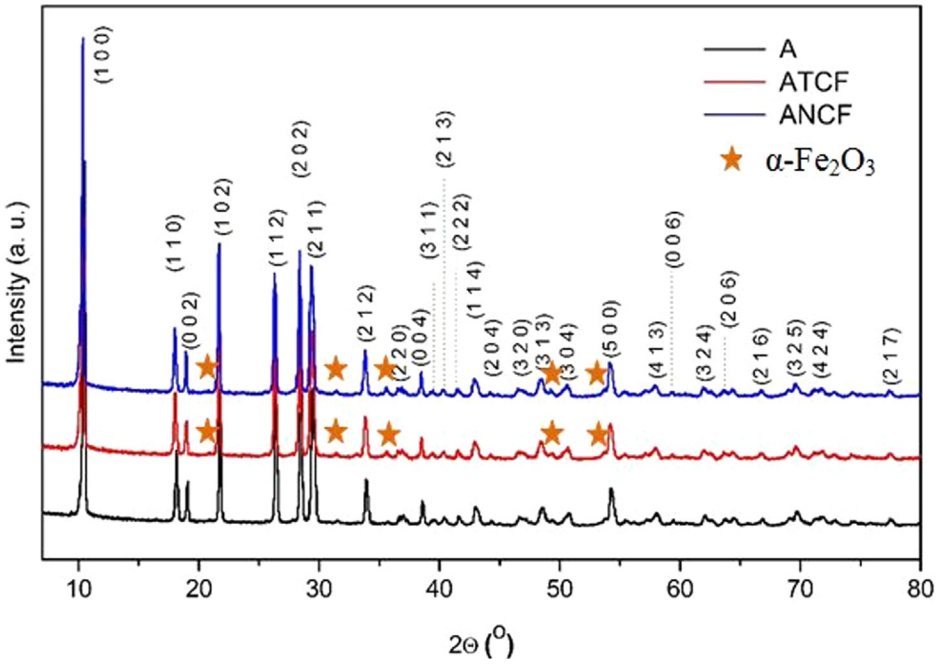

Fig. 7. XRD graph of A, ATCF and ANCF samples.

Table 3
BET surface area values and XRF analysis results.

		A	ATCF	ANCF
BET Surface Area (m^2/g)		114.230	44.649	50.104
Elements	**NaO**	0.146	0.163	0.160
	MgO	13.800	13.200	14.300
	Al_2O_3	34.100	32.900	33.900
	SiO_2	50.300	48.500	48.100
	P_2O_5	0.036	0.032	0.029
	SO_3	0.052	0.034	0.022
	K_2O	0.189	0.179	0.154
	CaO	0.321	0.217	0.201
	TiO_2	0.249	0.445	0.204
	Fe_2O_3	0.442	3.670	2.250
	Nb_2O_5	–	–	0.086
	CeO_2	–	0.045	0.174
	WO_3	0.312	0.585	0.429

CO and HC conversion rate. Therefore, maximum CO_2 increase rates and O_2 decrease rates of catalysts were obtained at the maximum engine torque in which maximum HC and CO conversions were occurred. However, at low engine loads, since the exhaust gas temperature is low, the change in O_2 and CO_2 content of exhaust gas were slight.

Fig. 11 displays the effect of catalyst on the exhaust gas temperature and smoke conversion efficiency. There was a linear relationship between the engine torque and amount of the temperature increase. The oxidation of CO and HC caused an increase in the exhaust gas temperatures. Compared to the ATCF, the temperature increase of ANCF was higher since its high CO and HC conversion. At the maximum engine torque in which maximum conversion rate was occurred, increase in temperature of exhaust gas were obtained as 34.25 °C for ATCF and 49.35 °C for ANCF.

However, DOC is widely used to reduce CO and HC emissions, it may also have an effect to eliminate smoke emissions [13,15]. DOC led

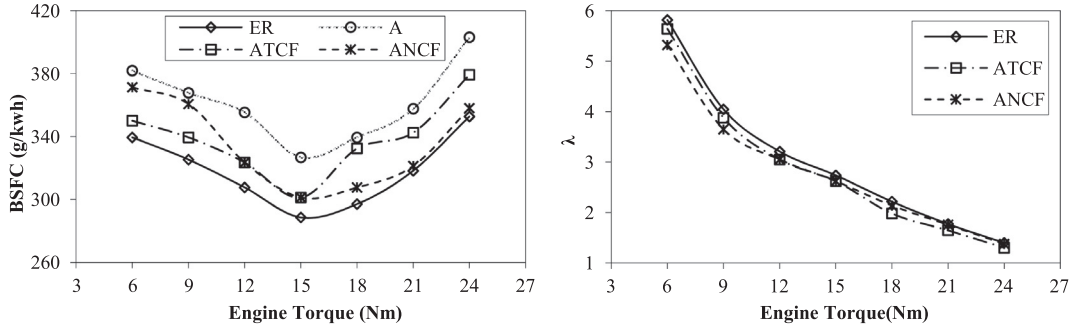

Fig. 8. The effect of catalysts on BSFC and λ.

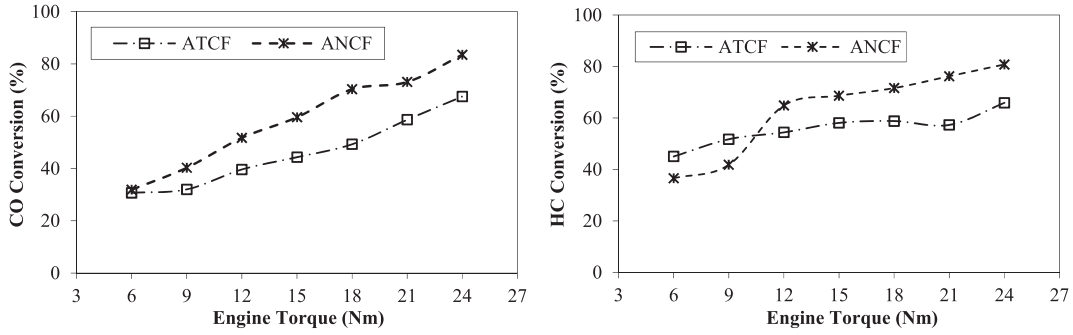

Fig. 9. The effect of catalysts on CO and HC emissions.

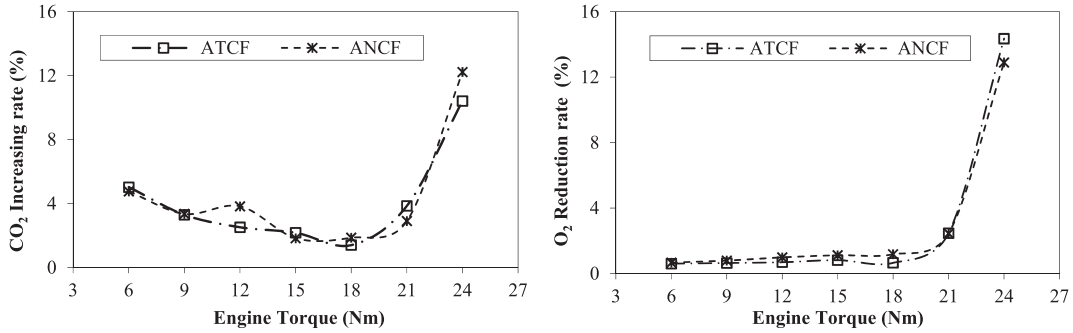

Fig. 10. The effect of catalysts on CO_2 emission and O_2 content.

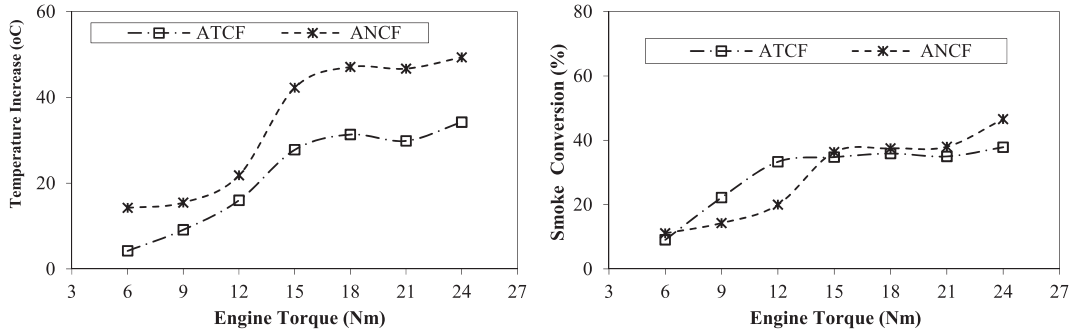

Fig. 11. The effect of catalysts on the exhaust gas temperature and smoke emission.

to the decrease in smoke emissions. The maximum decrease was obtained with ANCF as 46.61% at 24 Nm. ATCF resulted in a 37.84% decrease in this torque.

Conversion of NO to NO_2 form improves DPF and SCR activity. DPF efficiency is raised since NO_2 has more effective in converting PM than oxygen. When the amount of NO_2 in NO_x increases, the SCR reactions occur at a higher rate [13]. At the maximum engine torque, ATCF and ANCF catalysts raised the NO conversion to 62.24% and 76.08% respectively. ANCF performed better than ATCF in NO conversion. At 24 Nm, 334 ppm conversion in NO emission was occurred with ANFC catalyst.

The use of ATCF and ANCF as a SCR catalyst significantly decreased NO_x emissions (Fig. 12). The maximum decrease in NO_x emissions was obtained at the maximum engine torque, being 60.80% for ATCF and 80.29 for ANCF. The minimum NO_x emission obtained after ANCF catalyst was measured as 147 ppm with a reduction of 600 ppm at 24

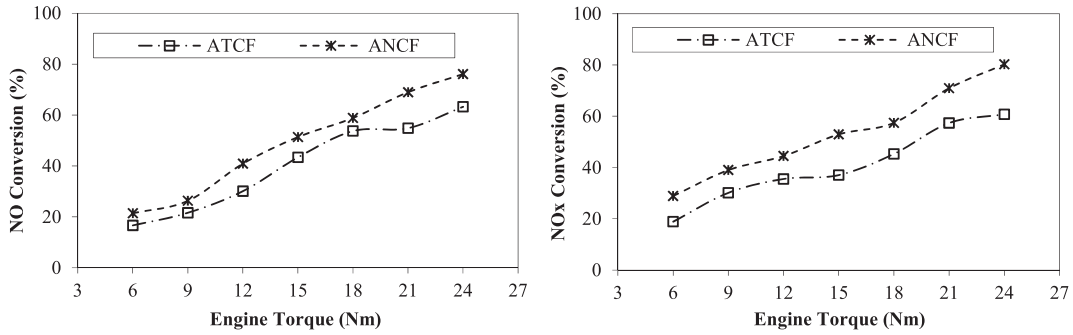

Fig. 12. The effect of the catalysts on NO and NO_x.

Nm. Compared to the ATCF catalyst, higher NO conversion rates of the ANCF catalyst provided better activity in NO_x conversion. Considering all the engine torques, ATCF catalyst led to 40.75% conversion rate while ANCF converted a little more, averagely 53.45% of NO_x emissions. The conversion rate increased in direct proportion to the increase of engine torque. Since the chemical reactions are kinetically limited at lower temperatures, lower conversion efficiencies were obtained at low engine torques [18].

4. Conclusion

In this study, we focused on the preparation of hematite-based catalysts by impregnation method and their effects on exhaust emissions as DOC and SCR catalyst. Based on the analyzes of catalysts and engine tests, the following conclusions were obtained:

- The pores of substrate were completely covered and a good ground was prepared for the catalyst works.
- The crystallite structure of the catalyst was a cordierite and had hexagonal structure with the space group of P6/mcc (1 9 2).
- Nb_2O_5 was more effective than TiO_2 in increasing crystallite structure.
- The CeO_2 rates in the ATCF and ANCF catalyst were 0.045% and 0.174% respectively. ANCF had Nb_2O_5 complex at a rate of 0.086%.
- The penetrating of catalyst materials in pores and sintering of catalyst structures led to the decrease in surface area of ANCF and ATCF compared to the main structure.
- The use of DOCs and SCR catalysts caused conversion of CO, HC, smoke and NO_x up to 83.51%, 80.83%, 46.61% and 80.29%, respectively.
- Because of oxidation reactions in DOC, O_2 concentration in exhaust gas decreased while CO_2 emissions increased.
- Catalyst use caused a slight increase in the BSFC of the engine and somewhat reductions in the λ values were observed.

Declaration of Competing Interest

The authors declare that they have no known competing financial interests or personal relationships that could have appeared to influence the work reported in this paper.

References

[1] Pietikainen M, Valiheikki A, Oravisjarvi K, Kolli T, Huuhtanen M, Niemi S, et al. Renewable Energy 2015;77:377–85.
[2] Guo J, Ge Y, Hao L, Tan J, Li J, Feng X. Atmos Environ 2014;99:1–9.
[3] Resitoglu İA, Altinisik K, Keskin A. Clean Techn Environ Policy 2015;17:15–27.
[4] Carslaw DC, Beevers SD, Tate JE, Westmoreland EJ, Williams ML. Atmos Environ 2011;45:7053–63.
[5] Ma Y, Zhu M, Zhang D. Appl Energy 2013;102:556–62.
[6] Shan W, Liu F, He H, Shi X, Zhang C. Catal Today 2012;184:160–5.
[7] Kumar P, Pirjola L, Ketzel M, Harrison RM. Atmos Environ 2013;67:252–77.
[8] Garcia-Perez J, Fernandez-Navarro P, Castello A, Lopez-Cima MF, Ramis R, Boldo E, et al. Environ Int 2013;51:31–44.
[9] Lopez JM, Jimenez F, Aparicio F, Flores N. Transp Res Part D 2009;14:1–5.
[10] Stepanek J, Koci P, Plat F, Marek M, Kubicek M. Comput Chem Eng 2010;34:744–52.
[11] Hauff K, Tuttlies U, Eigenberger G, Nieken U. Appl Catal B 2012;123–124:107–16.
[12] Zheng M, Banerjee S. Appl Therm Eng 2009;29:3021–35.
[13] Zhu L, Cheung CS, Zhang WG, Fang JH, Huang Z. Fuel 2013;113:690–6.
[14] Hamada H, Haneda M. Appl Catal A 2012;421–422:1–13.
[15] Vallinayagam R, Vedharaj S, Yang WM, Saravanan CG, Lee PS, Chua KJE, et al. Atmos Environ 2013;80:190–7.
[16] Baleta J, Vujanovic M, Pachler K, Duic N. J Cleaner Prod 2015;88:280–8.
[17] Can F, Courtois X, Berland S, Seneque M, Royer S, Duprez D. Catal Today 2015;257:41–50.
[18] Rauch D, Albrecht G, Kubinski D, Moos R. Appl Catal B 2015;165:36–42.
[19] Pang L, Fan C, Shao L, Yi J, Cai X, Wang J, et al. Chin J Catal 2014;35:2020–8.
[20] Ocakoglu K, Krupnik T, van den Bosch B, Harputlu E, Gullo MP, Olmos JDJ, et al. Adv. Funct. Mater. 2014;24:7467–77.